RSC Advances

ROYAL SOCIETY OF CHEMISTRY

www.rsc.org/advances

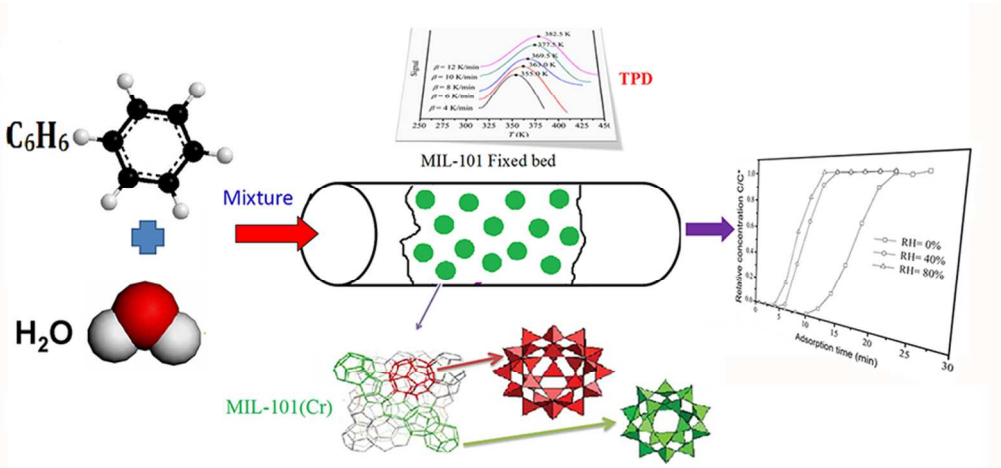

The existence of water vapor in the feed stream could led to a sharp decrease in the VOCs working capacity due to its strong competitive adsorption on the surfaces of MIL-101.

80x44mm (300 x 300 DPI)

Competitive Adsorption of water vapor with VOCs Dichloroethane, Ethyl Acetate and Benzene on MIL-101(Cr) in humid atmosphere

*Shikai Xian, Ying Yu, Jing Xiao, Zhijuan Zhang, Qibin Xia, Haihui Wang, Zhong Li**

School of Chemistry and Chemical Engineering, South China University of Technology, Guangzhou, 510640, China

* Corresponding author e-mail address: cezhli@scut.edu.cn

Abstract: It is well-known that water vapor is omnipresent. It would inevitably have negative influence on VOCs adsorption on novel porous materials in the cases of virtual situations. In this work, competitive adsorption behavior of water vapor with three VOCs such as 1,2-dichloroethane(DCE), ethyl acetate(EA) and benzene on MIL-101 in humid atmosphere were investigated by isotherm measurement, breakthrough experiments and TPD experiments. Results showed that adsorption capacities of MIL-101 for DCE, EA and benzene were separately up to 9.71, 5.79 and 3.76 mmol/g, much higher than those of other conventional adsorbents. Breakthrough experiments indicated that presence of water vapor in feed stream resulted in a sharp decrease in the VOCs working capacities of MIL-101 due to competitive adsorption of water vapor on MIL-101 surfaces. The breakthrough times and the working capacities of these VOCs became smaller with an increase in the relative humidity. TPD experiments indicated that the desorption activation energies of water vapor,

DCE, EA and benzene on MIL-101 were 72.9, 47.14, 41.9, and 38.16 kJ/mol, respectively. The stronger interaction of water vapor with MIL-101 formed strong competitive adsorption with VOCs on MIL-101, resulting in the sharp decrease of the VOCs working capacities in humid atmosphere.

Key words: Adsorption, TPD, breakthrough, MIL-101, water vapor, VOCs

1.Introduction

In recent decades, the release of anthropogenic toxic pollutants into the atmosphere is a worldwide threat of growing concern. Air pollution is now recognized as a severe problem and has become increasingly serious both nationally and worldwide[1]. Volatile organic compounds (VOCs) are the main pollutants in the ambient air released from chemical, petrochemical, and related industries. VOCs may cause short- and long-term adverse health risk for humans, such as headaches and eye, nose and throat irritation, dizziness, nausea, cancer, and even death even at very low concentrations. More and more countries and regions have proposed stringent legislations to impose stringent standards on VOC emissions from industries. Therefore, it is urgently needed to develop more safe and efficient systems for the removal of VOCs from polluted air.

There are many techniques available to abate the emission of VOCs, such as adsorption[2,3], catalytic oxidation[4], condensation[5], membrane separation[6] and biological treatments. Among these, adsorption method has been considered as one of the most cost-effective and environmentally friendly technologies for the removal of VOCs, especially at low concentration. Adsorbents play a key role in the adsorption

technique. Up to now, much work has been conducted to investigate the adsorption of VOCs on some traditional absorbents, such as activated carbon (AC), silica gel, activated alumina and zeolites. Although activated carbon and zeolites were widely applied for adsorption of VOCs, their disadvantages of the low capacity and difficulty in regeneration have limited its more wide application[7].

In recent years, a new class of porous materials assembled with metal ions and organic linkers, known as metal-organic frameworks (MOFs), has been rapidly developed as potential materials for VOCs adsorption due to their ultrahigh surface area, sturdy, open crystalline structure and adjustable chemical functionality [8, 9]. The presence of open metal sites (coordinatively unsaturated metal centers) or certain functionalizations on the pore surfaces of MOFs could enhance the adsorption selectivity/efficiency of MOFs towards certain toxic compounds via coordination bonds, acid–base/electrostatic interactions, p-complex/H-bonding formation, etc[8]. It is possible to take advantage of MOFs materials in order to develop new technologies for environmental remediation purposes. Barea et al.[8] reviewed performances of MOFs in environmental remediation processes, and their studies showed that some of MOFs and modified MOFs exhibited remarkable adsorption capacities and good selectivities of organic molecules. Among these MOFs, MIL-101(Matérial Institut Lavoisier, chromium-terphthalate-based solid) is considered as one of the most prominent representative in MOFs, which is basically built up from a hybrid superterahedral (ST) building unit, which is formed by rigid terephthalate ligands and trimeric chromium(III) octahedral clusters. It possesses a very large specific surface area with ordered micro/mesoporous zeotype architecture and high chemical and thermal stability[10]. Therefore, MIL-101 may become a promising candidate as an adsorbent for VOCs capture applications. Zhao et al.[11, 12] measured the adsorption

isotherms and kinetics of benzene and p-xylene on MIL-101, and reported that the maximum capacities of MIL-101 were 16.5 and 10.9 mmol/g at 288 K, respectively, much higher than activated carbons and zeolites. In addition, multiple cycle experiments of these VOCs Adsorption-Desorption on MIL-101 were carried out, and their results showed that efficiency of VOCs desorption can reach over 97%. Shi et al.[13] reported that the adsorption capacity of MIL-101 for ethyl acetate is up to 10.5 mmol/g at 288 K and 54 mbar. Diffusion coefficients of ethyl acetate within MIL-101 are in the range of (1.617 to 2.264)•10^{-10} cm ^{2}•s^{-1} with a lower activation energy of 8.361 kJ•mol^{-1}. In addition, multiple cycle experiments of these VOCs Adsorption-Desorption on MIL-101 were carried out, and results showed that desorption efficiency of VOCs can reach over 97%[11,13]. Thuyet al.[14] measured the isotherms of C6-C9 on MIL-101, and then reported that its maximum capacities for C6, C7, C8 and C9 reached about 9.95 , 8.82 , 8.75 and 6.17 mmol/g respectively.

Yang et al. [15]reported that MIL-101 had higher adsorption capacities for selected VOCs than zeolite, activated carbon and other reported adsorbents, and thus it was suitable for the adsorptive removal of VOCs including polar acetone and nonpolar benzene, toluene, ethylbeznene, and xylenes. Huang et al. [16] measured the isotherms of n-hexane, toluene, methanol, butanone, dichloromethane, and n-butylamine on MIL-101, and reported that MIL-101 had much higher affinity and adsorption capacity to VOCs than activated carbon, and its affinity to n-butylamine was the strongest among these VOCs. These studies above showed that the capacities of MIL-101 for VOCs were several times as that of the ACs, showing a great application prospect in the fields of environmental remediation and protection. However, if MIL-101 is used as a novel adsorbent applied in the actual cases, it will face the challenge of competitive adsorption of water vapor, which has not been studied yet.

It is well-known that water vapor is omnipresent. It often presents in various of polluted gases in the cases of virtual situations, and would commonly have negative influence on VOCs adsorption on adsorbents due to its strong competitive adsorption. The study on VOCs adsorption on MIL-101 in the presence of water vapor had hardly been done so far. Competitive adsorption behaviour and mechanism of water vapor and VOCs on MIL-101(Cr) in humid atmosphere has not been revealed yet. Therefore, it is necessary to investigate the effect of water vapor on VOCs adsorption on MIL-101 and its competitive adsorption mechanism so that some new knowledge can be obtained and adsorption process of MIL-101 for practical application of VOCs removal can be optimized or designed reasonably.

The purpose of this work is to investigate competitive adsorption behavior of water vapor and three VOCs EA, DCE and benzene on MIL-101 with the help of fixed bed experiments. Adsorption isotherms of EA, DCE, benzene and water vapor were separately measured by using a gravimetric method. The breakthrough curves of EA, DCE and benzene were measured under the conditions of the absence and the presence of water vapor, and then compared. TPD experiments were conducted to estimate the interaction of water vapor and VOCs EA, DCE and benzene with the surfaces of MIL-101. The competitive adsorption mechanism of water vapor with EA, DCE and benzene on MIL-101 would be discussed and then reported here.

2. Experimental section

2.1. Materials. Chromium(III) nitrate nonahydrate ($Cr(NO_3)_3 \cdot 9H_2O$, > 99.0%, Alfa), 1,4-benzene dicarboxylic acid ($C_8H_6O_4$, > 99.0%, Aldrich), hydrofluoric acid (HF, 48.0%, Merck) , *N*,*N*-dimethylformamide (DMF, 99.5%, Mallinckrodt), ethanol

(99.7%, Tianjin), NH_4F (≥ 96.0%, Tianjin), and 1,2-dichloroethane (≥ 99.0%,Tianjin). All of above were used as received from vendors without further purification.

2.2. Synthesis of MIL-101 and Characterization. The MIL-101 used in this work was synthesized by hydrothermal method and the specific are described in supporting information (S1).

The surface morphology and particle size of MIL-101 samples were observed by using a LEO 1530Vp scanning electron microscope (SEM) at an accelerating voltage of 5.0 kV after gold deposition. The synthesized MIL-101 was characterized by X-ray powder diffraction (XRD), which was performed on Bruker D8 Advance X-ray diffractometer at 40 kV, 40 mA, with a scan speed of 2°/min and a step size of 0.02° in 2 ~25 , using λ_{Cu} Kα radiation. Specific surface area and pore texture of the sample were measured using Micromeritics ASAP 2020.

2.3. Measurement of Adsorption Isotherms of DCE, EA and benzene Vapor. Adsorption isotherms of DCE, EA and benzene vapor on MIL-101 sample were measured by using a standard gravimetric technique (intelligent gravimetric analyzer, IGA-003, Hiden) at 298-318 K. This intelligent gravimetric analyzer (IGA-003, Hiden) is equipped with an ultra-sensitive balance of resolution 0.2 μg. Details of the measurement procedures can be available in the supporting information (S2). The equilibrium and instantaneous uptakes of DCE, EA and benzene on the sample can be calculated as follows:

$$Q_e = \frac{1000(W_e - W_a)}{W_a M_{DCE}} \quad (1)$$

$$Q_t = \frac{1000(W_t - W_a)}{W_a M_{DCE}} \quad (2)$$

where M_{DCE} (g/mol) is the molecular weight of VOC molecule; W_e(g) and W_t(g) are the amount of adsorbent (the MIL-101) at equilibrium and time t(s); W_a(g) is the initial weight of the sample (MIL-101); and Q_e (mmol/g) and Q_t (mmol/g) are the VOC amount adsorbed per gram of adsorbent at equilibrium and at time t(s), respectively(S2).

2.4. Measurement of Adsorption Isotherms of Water Vapor. Isotherm of water was measured on Gravimetric water sorption analyzer (AQVADYNE DVS) equipped with a microbalance with an accuracy of 1μg. Details of the measurement procedures can be available in the supporting information (S2).

2.5. Temperature Programmed Desorption Experiments. Temperature programmed desorption (TPD) is an effective technique of surface analysis[11]. In this work, TPD experiments were conducted to estimate the binding energy between an adsorbate and an adsorbent. The detailed description of methods for TPD experiment and estimation of desorption activation energy are given in supporting information (S3).

2.6. Determination of Breakthrough Curves under Different Relative Humidities. Fixed bed adsorption experiments were conducted at 308 K to measure the breakthrough curves of DCE, EA and benzene on MIL-101 under the conditions of relative humidities of 5%, 40%, and 80%, separately. The experimental setup is a flow-typed fixed-bed adsorption system, which is shown in Supporting Information (Fig. S1) and the detailed description of the method is given in Supporting Information (S4).

3. Result and Discussion

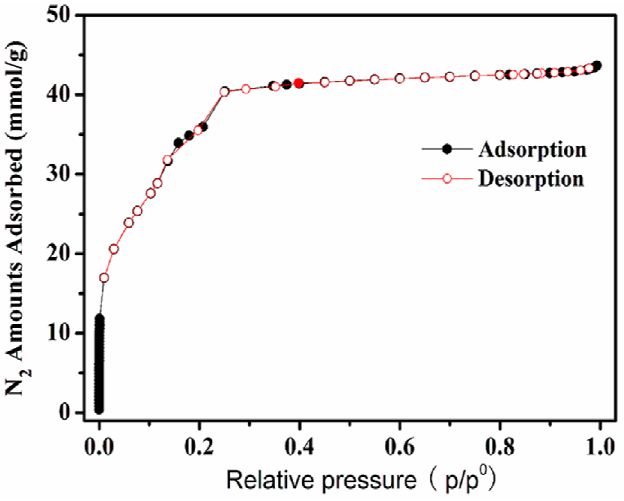

Fig. 1. Adsorption- desorption isotherms of N_2 on MIL-101 at 77 K.

3.1. Sample Characteristics. Fig. 1 shows the nitrogen adsorption and desorption isotherms of MIL-101 sample. It can be seen that the N_2 isotherm on MIL-101 was of typical type-V profile with secondary uptakes, which is characteristic of the presence of the two kinds of microporous[10]. Textural properties of sample can be obtained from the isotherm by analyzing the nitrogen adsorption and desorption isotherms with the Micromeritics ASAP 2010 built in software. The BET specific surface area and total pore volume of MIL-101 synthesized in this work were 3360 m^2/g and 1.75 cm^3/g, respectively. In addition, the SEM image and XRD pattern of the sample are also obtained, which can be seen in Supporting Information (S5, Fig. S2 and S3).

3.2. Isotherms of Three VOCs on MIL-101. Fig. 2 presents the isotherms of DCE, EA, and benzene on MIL-101 at 308 K. It shows that the isotherms of DCE and EA were favorable ones, while the isotherm of benzene was an unfavorable isotherm. The isotherms of DCE and EA were higher than that of benzene, suggesting that the adsorption capacity of MIL-101 for DCE or EA was higher than that for benzene. The amounts adsorbed of DCE, EA and benzene on MIL-101 followed the order: DCE >

EA > benzene. For example, at 8 mbar, the adsorption capacity of MIL-101 for DCE was up to 9.7 mmol/g, that for DCE was about 5.5 mmol/g, and that for DCE was about 3.3 mmol/g. This difference in adsorption capacity may be ascribed to the different polarity of the three VOCs molecule. DCE and EA are polar molecules whose dipole moments are 1.8D and 1.78D respectively. Benzene is non-polar molecule with dipole moments of zero. The different polarities of the three VOCs molecule result in the different interactions between VOC molecules and the framework of MIL-101 sample. As a result, the isotherms of DCE and EA were favorable ones due to their strong adsorption, while the isotherm of benzene was an unfavorable isotherm due to its weaker adsorption compared to DCE and EA. In addition, Table 1 gives the comparison between adsorption capacities of MIL-101 and some other porous materials for DCE, EA and benzene at similar conditions. It indicated that the adsorption capacities of MIL-101 were much higher than those of the other materials.

Langmuir and Freundlich equations were applied to fit the experimental isotherm data in order to describe adsorption behavior of DCE, EA and benzene on MIL-101 sample, as shown in Fig. 2. The Langmuir equation seems to give a good fit to the experimental isotherm data of DCE and EA. However, the Langmuir equation was not fit for adsorption data of benzene, but the Freundlich equations can give a good fit.

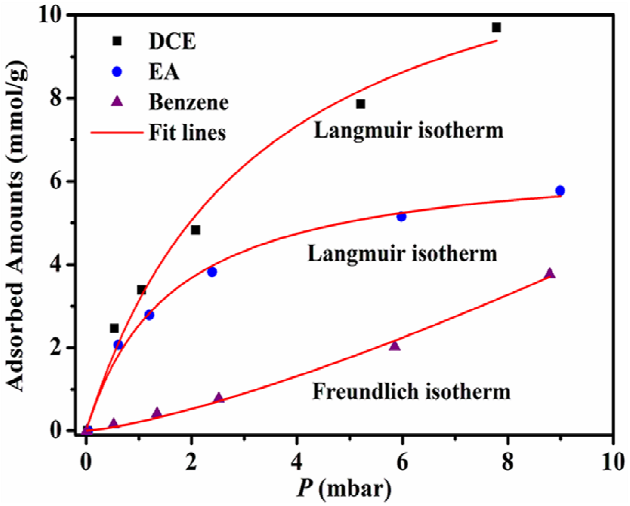

Fig. 2. Adsorption isotherms of DCE, EA and Benzene on the MIL-101 at low pressure and 308 K (points, experimental data; solid curves, fitted isotherm with Langmuir/Freundlich equation).

196

197 **Table 1. The Adsorption Capacities of MIL-101 and some other Materials for DCE, EA and**

198 **Benzene**

VOC	Material	Q (mmol/g)	T (K)	Pressure(mbar)	Reference
DCE	MIL-101	9.7	308	8	Present work
	LC-1	3	303	8	[17]
	HC-MWCNTs	0.05	323	8	[18]
EA	MIL-101	5.5	308	8	Present work
	MCM-48	1	293	8	[19]
	HDTMA clay	0.4	308	8	[20]
benzene	MIL-101	3.3	308	8	Present work
	MOF-5	0.8	303	8	[21]
	silicalite-1	1	295	8	[22]
	H-ZSM-5	1.3	303	8	[23]
	SBA-15	0.83	303	8	[23]

199

200 The fitting parameters of Freundlich isotherm and Langmuir isotherm equations as

201 well as their linear correlation coefficients (R^2) were listed in Supporting Information

(Table S1). Examination of the data shows that the Langmuir and Freundlich equations were able to fit the experimental adsorption data well since their correlation coefficients R^2 were up to 0.99.

3.3. Effects of Water Vapor on Breakthrough Curves of VOCs through the Fixed Bed of MIL-101. Figs. 3-5 show the adsorption breakthrough curves of DCE, EA, and benzene through the fixed bed packed with MIL-101 at different relative humidity, separately. It was clearly visible that the relative humidity of feed stream containing VOCs had negative influence on the breakthrough curves of these VOCs in the packed bed. The breakthrough times of these VOCs sharply decreased with an increase in the humidity of the feed stream, implying that the working adsorption capacity of MIL-101 sharply decreased due to presence of water vapor in the feed stream. The higher relative humidity would make the breakthrough times of the VOCs become shorter.

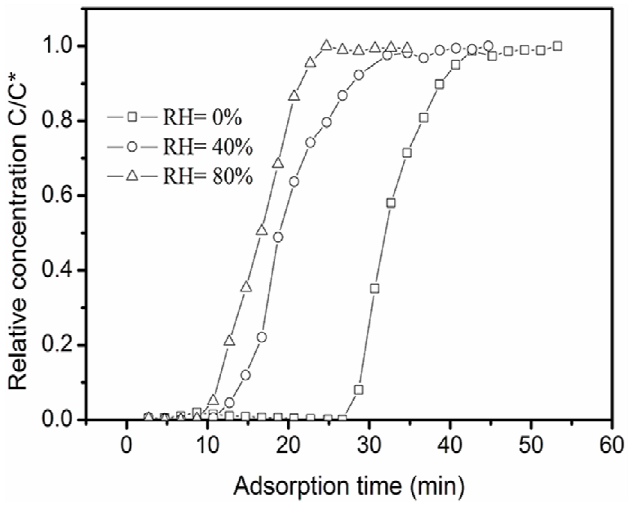

Fig. 3. Effect of relative humidity on the breakthrough curves of EA through the fixed bed of the MIL-101 (T=308 K, N_2 flow rate= 70 ml/min).

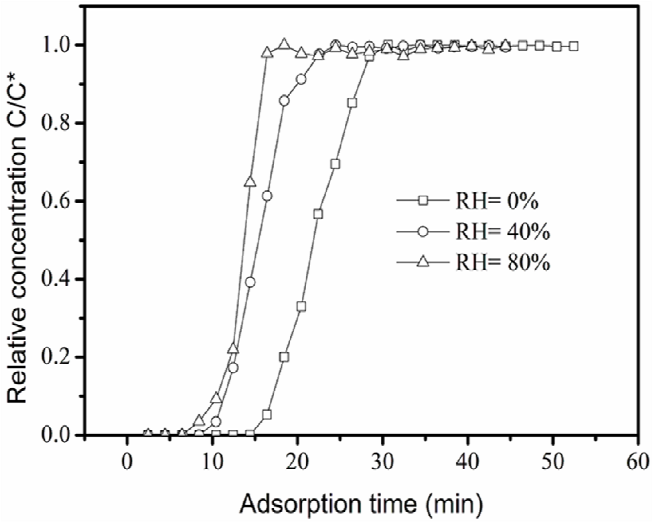

Fig. 4. The effect of relative humidity on the breakthrough curves of DCE through the fixed bed of the MIL-101(*T*=308 K, N_2 flow rate= 70 ml/min).

217

218

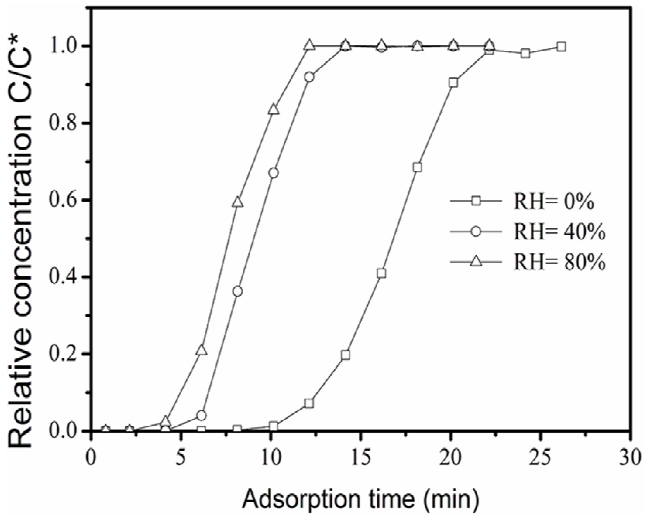

Fig. 5. Effect of relative humidity on the breakthrough curves of Benzene through the fixed bed of the MIL-101 (*T*=308 K, N_2 flow rate= 70 ml/min).

219

220 **Table 2. Effects of Relative Humidity on Breakthrough Times and Working**
221 **Capacities of DCE， EA and Benzene Adsorption on MIL-101 at 308 K.**

Adsorbate	C_0 (mol/L)	RH (%)	Breakthrough time (min)	Working capacity (mmol/g)

DCE	5×10^{-5}	5	16.3	2.282
		40	10.7	1.498
		80	8.9	1.246
EA	2×10^{-5}	5	27.9	1.562
		40	12.8	0.717
		80	10.6	0.594
BE	10^{-5}	5	11.4	0.319
		40	6.24	0.175
		80	4.46	0.125

Table 2 lists the breakthrough times and working adsorption capacities of EA, DCE and Benzene on MIL-101 under the conditions of different relative humidities. It indicated that the breakthrough times and the working capacities of these VOCs became smaller with an increase in the relative humidity. When the relative humidity of the feed stream increased from 0% to 80%, the VOCs breakthrough times or the working adsorption capacities were decreased by about 45, 62 and 60.8% separately for DCE, EA, and benzene. It could be attributed to the competition adsorption of water vapor on the surfaces of MIL-101. MIL-101 is amphiphilic porous solids since its framework is composed of inorganic (metal cations and oxygen anions) and organic moieties (nonpolar carbon atoms and benzene ring)[23, 24]. Thus it has polar sites due to the metal oxygen clusters and very non-polar regions due to the presence of organic and mostly aromatic linker[23]. In dry condition, the unsaturated Cr^{3+} sites on MIL-101 were also the strong adsorption site for VOCs[11]. In the case of the presence of water vapor in adsorption system, H_2O molecules preferably adsorbed on the hydrophilic centers such as trivalent metal cations[25], and then if the concentration of

water vapor became higher further additional water molecules are bound by hydrogen bridges to these water nucleation sites resulting in small water clusters[23, 26]. As a result, the part surface area of MIL-101 would be occupied by more H_2O molecules, and thus the less adsorptive sites are available for adsorption VOCs. In fixed bed adsorption experiment, when the gaseous mixture containing VOCs and water vapor passed the fixed bed of MIL-101, some water molecules preferentially adsorbed on the hydrophilic centers such as Cr^{3+}sites of MIL-101, and thus the surface active sites of MIL-101 for adsorption VOCs became less. As a consequence of that, the working adsorption capacity of the fixed bed of MIL-101 for VOCs would greatly decrease due to competitive adsorption of water molecules.

Figs. 6a-6c show a comparison of breakthrough curves of benzene at different temperatures in the presence and absence of water vapor. It was observed from Fig. 6 that breakthrough times of benzene in the presence and absence of water vapor decreased obviously as temperature rose. It can be attributed to a decrease in adsorption capacity of MIL-101 for benzene due to rising of temperature, as shown in Fig.S6. In addition, it was noticed that the breakthrough times in the presence of water vapor was always shorter than in the absence of water vapor at different temperatures. It meant that although the rise of temperature could weaken adsorption of water vapor on MIL-101, there was still the negative effect of water vapor on benzene adsorption on MIL-101 in the range of temperatures studied.

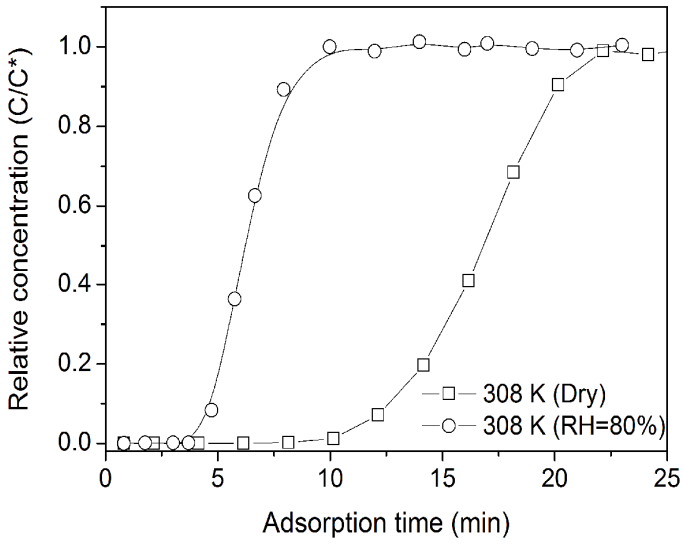

Fig. 6a. The breakthrough curves of benzene on MIL-101 at 308 K.

258

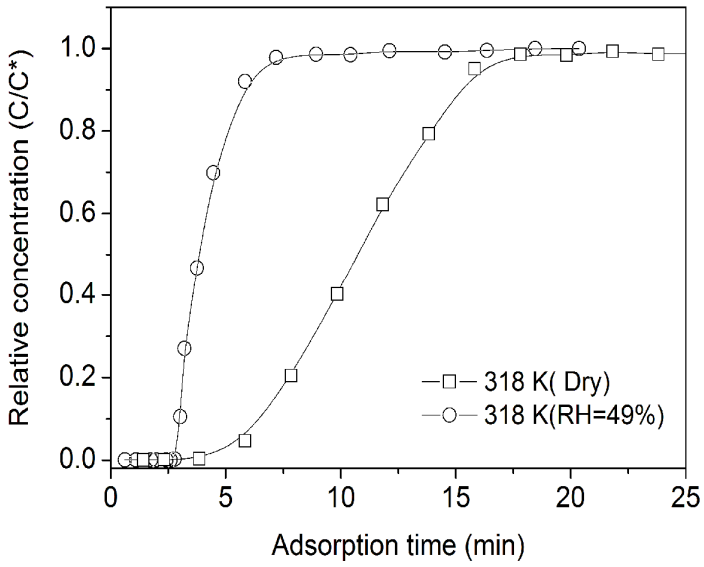

Fig. 6b. The breakthrough curves of benzene on MIL-101 at 318 K.

259

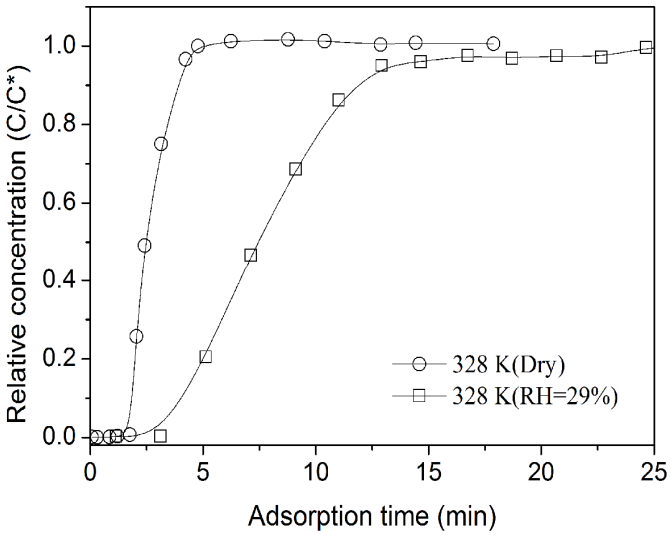

Fig. 6c. The breakthrough curves of benzene on MIL-101 at 328 K.

260

261 **3.4. Isotherm of Water Vapor on MIL-101.** Fig. 7 shows the adsorption isotherm
262 of water vapor on MIL-101 at 308K. It exhibited an S-shaped type of the isotherm
263 with maximum water vapor uptake of 83 mmol/g. The amount adsorbed of H_2O vapor
264 was low at the relative humidity below 30%, and then sharply increased when the
265 relative humidity reaching 40 RH%. As the relative humidity increased, the amount
266 adsorbed of water vapor water continued to rise.

267

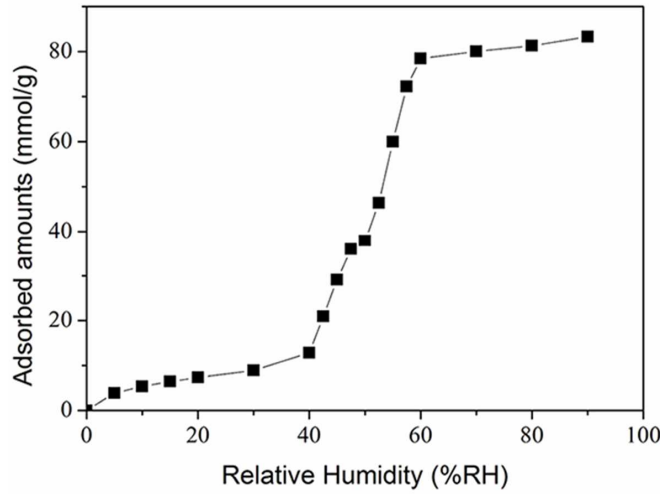

Fig. 7. The adsorption isotherm of water vapor on the MIL-101.

268

269 **3.5. Desorption Activation Energies of the VOCs and H_2O vapor on MIL-101.**

270 Fig. 8 shows a series of TPD curves of EA, DCE and benzene on MIL-101 at different
271 heating rates. Each of these TPD curves exhibited one peak due to EA, DCE or
272 benzene desorption, and its peak temperature (T_p) increased with an increase in
273 heating rate.

274

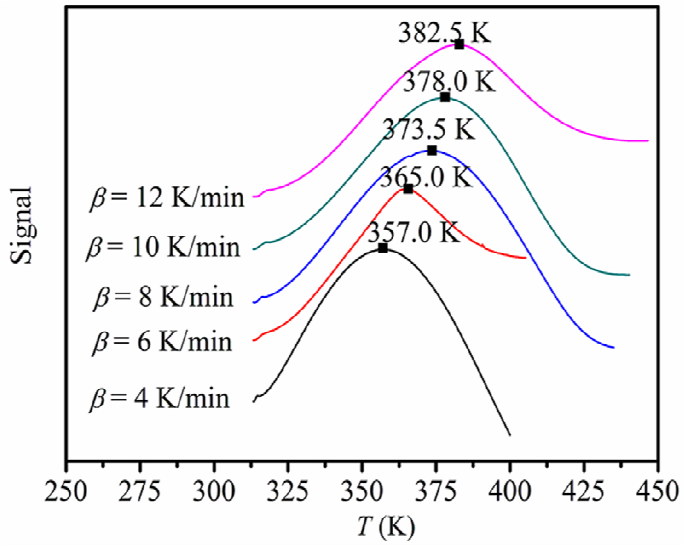

Fig. 8a. TPD spectrums of EA on MIL-101 at different heating rate from 4-12 K/min.

275

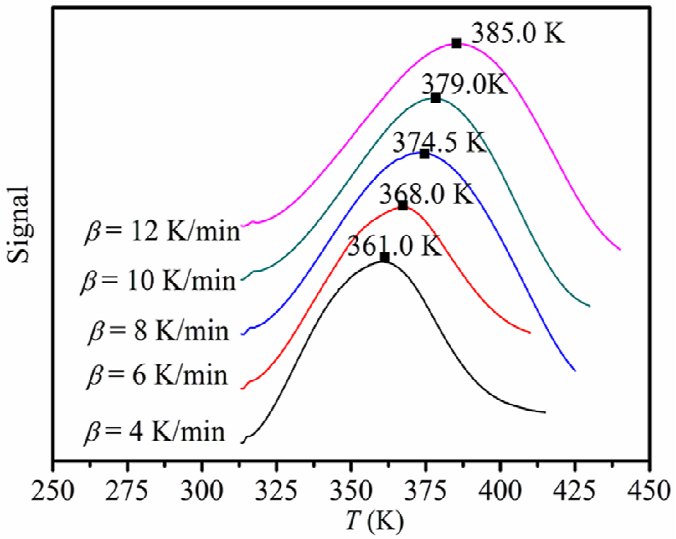

Fig. 8b. TPD spectrums of DCE on MIL-101 at different heating rate from 4-12 K/min.

276

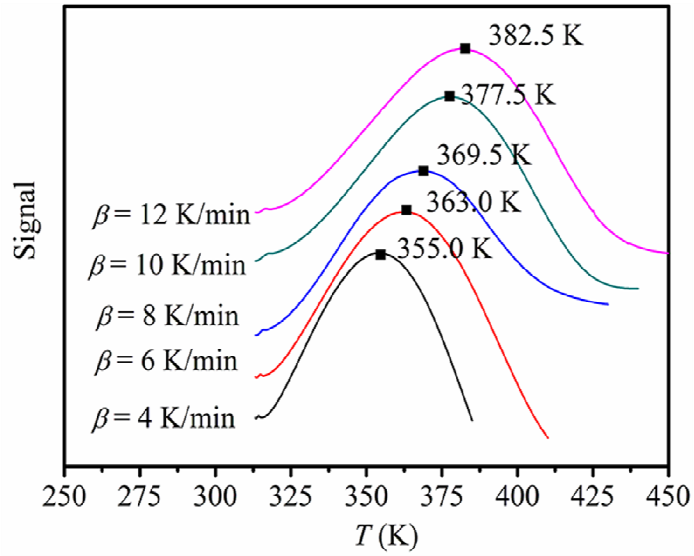

Fig. 8c. TPD spectrums of benzene on MIL-101 at different heating rates from 4-12 K/min.

277

278 Knowing the values of T_p at the different heating rates employed (in Table 3),

279 desorption activation energy of EA, DCE or benzene can be estimated by using

Polanyi-Wigner equation (See Supporting Information S2 and Fig.S4). Calculation indicated that desorption activation energies of the three VOCs on MIL-101 were 47.14, 41.9, and 38.16 kJ/mol, respectively, which followed the order: DCE > EA > benzene.

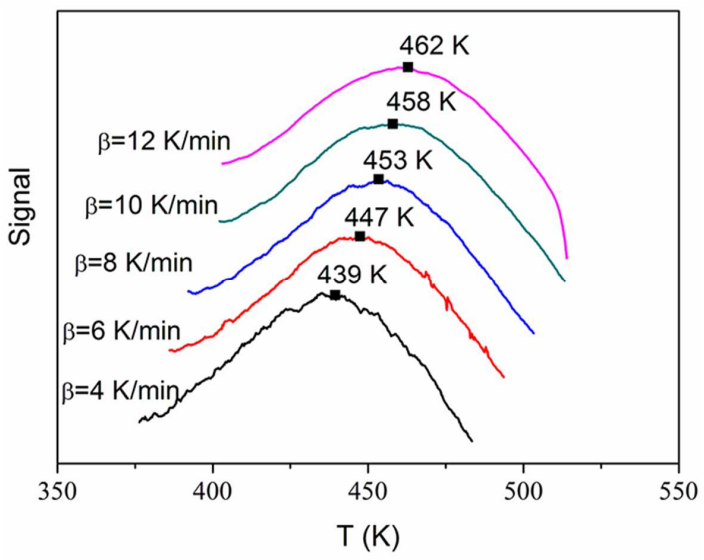

Fig. 9. TPD spectrums of H_2O vapor on the MIL-101 at different heating rates from 4-12 K/min.

Table 3 Desorption activation energies of EA, DCE, Benzene, and H_2O on the MIL-101.

VOCs	T_p (K)					E_d (kJ/mol)	R^2
	4 K/min	6 K/min	8 K/min	10 K/min	12 K/min		
EA	357	365	373.5	378	382.5	41.9	0.997
DCE	361	368	374.5	379	385	47.14	0.995
Benzene	355	363	369.5	377.5	382.5	38.16	0.993
H_2O	439	447	453	458	462	72.96	0.999

In similar manner, TPD experiments were also conducted for water vapor at different heating rates. Fig. 9 exhibits the TPD spectrums of water vapor desorption from MIL-101 at different heating rates (Table 3). It was clearly visible that only one peak appeared in each of their TPD curves, and the peak temperature (T_p) increased with an increase in heating rate. In similar method mentioned above, the desorption activation energy of water vapor on MIL-101 was estimated to be 72.9 kJ/mol (See Supporting Infomation Fig. S5), which was higher than that of the three VOCs. The higher desorption activation energy meant a stronger interaction between H_2O molecules and the surfaces of MIL-101 compared to those three VOCs. This would make the presence of water vapor in the feed stream result in a sharp decrease in the VOCs working adsorption capacities of MIL-101 due to strong competitive adsorption of water vapor on the surfaces of MIL-101.

4. Conclusion

Adsorption behavior of 1,2-dichloroethane(DCE), ethyl acetate(EA), and Benzene in the fixed bed of MIL-101 was investigated in the presence of water vapor. The results showed that the equilibrium amounts adsorbed of DCE, EA and benzene on MIL-101 followed the order: DCE > EA > benzene. The maximum adsorption capacities of MIL-101 for DCE, EA and benzene were separately up to 9.71, 5.79 and 3.76 mmol/g, being much higher than those of some other adsorbents such as zeolites, activated carbons and clay. The presence of water vapor in the feed stream had remarkable negative influence on the breakthrough behavior of VOCs in the fixed bed. The breakthrough times and the working capacities of these VOCs became smaller with an increase in the relative humidity. Isotherm of water vapor on MIL-101 at 308 K exhibited an S-shaped type of the isotherm, which can be expressed by DSLF

model. TPD experiments showed that the desorption activation energies of water vapor, DCE, EA and benzene on MIL-101 followed the order: water vapor > DCE > EA > benzene, which were 72.9, 47.14, 41.9, and 38.16 kJ/mol, respectively. The higher desorption activation energy of water vapor suggested the interaction between water molecule and MIL-101 was stronger than that between DCE, EA, or benzene and MIL-101. The stronger interaction of water vapor with MIL-101 formed stronger competitive adsorption with VOCs on MIL-101. As a result, the existence of water vapor in the feed stream could led to a sharp decrease in the working adsorption capacity of MIL-101 for these VOCs due to its strong competitive adsorption on the surfaces of MIL-101. Getting well-understanding of water vapor impact on the VOCs adsorption on the MOFs under humid atmosphere would be helpful to design reasonably adsorption process or study novel hydrophobic materials. Thus, an interesting topic or a challenge topic will appear. Therefore, the preparation of hydrophobic MOFs by surface modification for enhancing their adsorption of VOCs in the practical application would be worthy of investigation in the future.

ACKNOWLEDGMENT

This work was supported by National Natural Science Foundation of China (No. 21436005 and No. 21376090), National Science Fund for Distinguished Young Scholars of China (No. 21225625), the Science Foundation of Guangzhou City, the Fundamental Research Funds for the Central Universities, and the State Key Lab of Subtropical Building Science (Grant C714004z).

Reference

1. Zhu, X. B.; Gao, X.; Zheng, C. H. Wang , Z. H.; Ni, M. J.; Tu, X., *RSC Adv.*, 2014,**4**, p 37796-37805

2. Zhang, S. J.; Shao, T.; Kose, H. Selcen; Tanju, Karanfil, *Environ. Sci. Technol.*, 2010, **44**, (16), p 6377-6383

3. Chen, Y. S.; Hsu, Y. C.; Lin, C. C.; Tai, C. Y. D.; Liu, H. S., *Environ. Sci. Technol.*, 2008, **42**, (7), 2631-2636.

4. Fang, J. C.; Chen, X.; Xia, Q. B.; Xi, H. X.; Li, Z., *Chin. J. Chem. Eng.*, 2009, **17**, (5), 767-772.

5. Zaitan, H.; Bianchi, D.; Achak, O.; Chafik, T., *J. Hazard. Mater.*, 2008, **153**, (1-2), 852-859.

6. Zhen, H. F.; Jang, S. M. J.; Teo, W. K.; Li, K., *J. Appl. Polym. Sci.*, 2006, **99**, (5), 2497-2503.

7. Qi, N.; Appel, W. S.; LeVan, M. D.; Finn, J. E., *Ind. Eng. Chem. Res.*, 2006, **45**, (7), 2303-2314.

8. Barea, E.; Montoro, C.; Navarro, J. A. R., *Chemical Society Reviews* 2014, **43**, (16), 5419-5430.

9. Eddaoudi, M.; Kim, J.; Rosi, N.; Vodak, D.; Wachter, J.; O'Keeffe, M.; Yaghi, O. M., *Science*, 2002, **295**, (5554), 469-472.

10. Férey, G.; Mellot-Draznieks, C.; Serre, C.; Millange, F.; Dutour, J.; Surblé, S.; Margiolaki, I., *Science*, 2005, **309**, (5743), 2040-2042.

11. Zhao, Z. X.; Li, X. M.; Huang, S. S.; Xia, Q. B.; Li, Z., *Ind. Eng. Chem. Res.*, 2011, **50**, (4), 2254-2261.

12. Zhao, Z.; Li, X.; Li, Z., *Chem. Eng. J.*, 2011**, 173**, (1), 150-157.

13. Shi, J.; Zhao, Z.; Xia, Q.; Li, Y.; Li, Z., *J. Chem. Eng. Data*, 2011**, 56**, (8), 3419-3425.

14. Trung, T. K.; Ramsahye, N. A.; Trens, P.; Tanchoux, N.; Serre, C.; Fajula, F.; Férey, G., *Micropor. Mesopor. Mat.*, 2010, **134**, (1–3), 134-140.

15. Yang, K.; Sun, Q.; Xue, F.; Lin, D., *J. Hazard. Mater.*, 2011, **195**, (0), 124-131.

16. Huang, C.-Y.; Song, M.; Gu, Z.-Y.; Wang, H.-F.; Yan, X.-P., *Environ. Sci. Technol.*, 2011**, 45**, (10), 4490-4496.

17. Long, C.; Liu, P.; Li, Y.; Li, A. M.; Zhang, Q. X., *Environ. Sci. Technol.*, 2011, **45**, (10), 4506-4512.

18. Sone, H.; Fugetsu, B.; Tsukada, T.; Endo, M., *Talanta*, 2008, **74**, (5), 1265-1270.

19. Wu, S.; Wang, J.; Liu, G.; Yang, Y.; Lu, J., J. *Membr. Sci.*, 2012, **390–391**, (0), 175-181.

20. Cavalcante, A. M.; Torres, L. G.; Coelho, G. L. V., *Braz. J. Chem. Eng.*, 2005, **22**, 75-82.

21. Shim, W.-G.; Hwang, K.-J.; Chung, J.-T.; Baek, Y.-S.; Yoo, S.-J.; Kim, S.-C.; Moon, H.; Lee, J.-W., *Adv. Powder Technol.*, 2012, **23**, (5), 615-619.

22. Song, L.; Sun, Z.-L.; Ban, H.-Y.; Dai, M.; Rees, L. V. C., *Phys. Chem. Chem. Phys.*, 2004, **6**, (19), 4722-4731.

23. Jhung, S. H.; Lee, J. H.; Yoon, J. W.; Serre, C.; Ferey, G.; Chang, J. S., *Adv. Mater.*, 2007, **19**, (1), 121-124.

24. Akiyama, G.; Matsuda, R.; Sato, H.; Hori, A.; Takata, M.; Kitagawa, S., *Micropor. Mesopor. Mat.*, 2012**, 157**, (0), 89-93.

25. Küsgens, P.; Rose, M.; Senkovska, I.; Fröde, H.; Henschel, A.; Siegle, S.; Kaskel, S., *Micropor. Mesopor. Mat.*, 2009, **120**, (3), 325-330.

26. Seo, Y.-K.; Yoon, J. W.; Lee, J. S.; Hwang, Y. K.; Jun, C.-H.; Chang, J.-S.; Wuttke, S.; Bazin, P.; Vimont, A.; Daturi, M.; Bourrelly, S.; Llewellyn, P. L.; Horcajada, P.; Serre, C.; Férey, G., *Adv. Mater.*, 2012, **24**, (6), 806-810.